JOURNAL OF MATERIALS SCIENCE 33 (1998) 1759–1763

Growth of nano-α-Fe_2O_3 in a titania matrix by the sol–gel route

T. K. KUNDU, M. MUKHERJEE, D. CHAKRAVORTY*
Indian Association for the Cultivation of Science, Jadavpur, Calcutta 700032, India,
**and also Jawaharlal Nehru Centre for Advanced Scientific Research, Bangalore 560012, India*

T. P. SINHA
Department of Physics, Bose Institute, 93/1, Acharya Prafulla Chandra Road, Calcutta 700009, India

Nano-α-Fe_2O_3 in a titania matrix was prepared by the sol–gel route. The nanocomposites containing various sizes of α-Fe_2O_3 were precipitated by the heat treatment of the dried gel in a temperature range 100–1200 °C. Differential thermal analysis of the TiO_2–Fe_2O_3 system showed peaks at 325, 390 and 730 °C. The formation of anatase as well as the rutile phase of TiO_2 and the growth of α-Fe_2O_3 were predicted from the above peak analysis. These results were in agreement with the X-ray diffraction studies. The sizes of the nanoparticles were analysed by transmission electron microscopic studies. The Mössbauer spectra of TiO_2–Fe_2O_3 nanocomposites showed paramagnetic and superparamagnetic doublets for all the specimens containing nanoparticles of α-Fe_2O_3. The electron paramagnetic resonance study indicated the presence of a paramagnetic phase in the nanocomposite samples.

1. Introduction

Nanocomposite materials have recently been studied extensively [1–6] because of their potential use in technology, such as high-density magnetic recording media, ferrofluids, catalysts, and so on. Various techniques, such as vapour deposition [7], r.f. sputtering [8], reducing from metal oxide [9], hydrothermal precipitation [10], etc., have been employed to prepare ultrafine particles. Among the variety of means to prepare nanocomposite materials, the sol–gel method has already proved to be an effective and economical way of fabrication [11, 12]. The improved characteristics of these materials are, in fact, due to the presence of a very large number of grain interfaces. Recently, we have made a systematic study of the growth of nanosized α-Fe_2O_3 in a silica glass matrix prepared by the sol–gel route [13]. The Mössbauer spectrum of the dispersed system of magnetic nanocrystals is a superposition of a Zeeman sextet corresponding to large-size ferromagnetic particles and a superparamagnetic doublet, corresponding to particles of smaller size [13]. Such characteristic features of the nanoparticles are dependent on the heat treatment of the gel. It has thus been possible to study the growth kinetics of nano-α-Fe_2O_3 in various glass matrices. In the present study, we report the preparation of the Fe_2O_3–TiO_2 nanocomposite system by sol–gel method and its investigation by several measurement techniques. The crystallographic structures of the samples were determined by X-ray diffractrometry (XRD) and differential thermal analysis (DTA). Transmission electron microscopy (TEM) observations were performed to determine the particle-size distribution. The room-temperature Mössbauer spectra were obtained and the electron paramagnetic resonance (EPR) spectra were recorded. To our knowledge, this is the first time that the growth of nano-α-Fe_2O_3 in a titania matrix by the sol–gel route has been reported.

2. Experimental procedure

The composite system investigated was TiO_2–Fe_2O_3. The precursor compounds used for preparation of the samples were $FeCl_3 \cdot 6H_2O$ and $C_{12}H_{28}O_4Ti$ (tetra-isopropyl orthotitanate). First, a sol (a) of titania was prepared by the hydrolysis of 10 ml tetra-isopropyl orthotitanate in a 40 ml mixture of acetic acid and ethyl alcohol in a volume ratio of 25:75. Mixture (a) was stirred for 1 h. Another solution (b) of 0.6 g $FeCl_3 \cdot 6H_2O$ in 10 ml water was prepared and poured into mixture (a). The resulting mixture was then stirred for 1 h to get the final sol. The sol was then kept at room temperature for 72 h for gelation. The gel was then slowly heated in a controlled oven up to 100 °C and was kept there for 7 d. The gel was divided into several parts. For the precipitation of Fe_2O_3 the gel pieces were subjected to the scheduled heat treatment summarized in Table I.

TABLE I Summary of heat-treatment schedule for specimens in the TiO_2–Fe_2O_3 system

Heat treatment	Sample	Phase identified by X-ray	Phase identified by TEM
200 °C/2 h	A	Anatase TiO_2	Anatase TiO_2
300 °C/2 h	B	Anatase TiO_2	Anatase TiO_2
400 °C/2 h	C	Anatase TiO_2	Anatase TiO_2
600 °C/2 h	D	Anatase TiO_2	Anatase TiO_2
800 °C/2 h	E	Rutile TiO_2 and α-Fe_2O_3	Rutile TiO_2 and α-Fe_2O_3
1000 °C/2 h	F	Rutile TiO_2 and α-Fe_2O_3	Rutile TiO_2 and α-Fe_2O_3
1150 °C/2 h	G	Rutile TiO_2 and α-Fe_2O_3	Rutile TiO_2 and α-Fe_2O_3

The DTA analysis of the 100 °C (oven dried) gel was carried out in a Shimadzu DT–40 thermal analyser at a heating rate of 5 °C min^{-1} with a sensitivity of 20 μV in^{-1}.

The X-ray analyses of all the samples were performed in a Phillips PW 1877 apparatus using CuK_α radiation.

The microstructures of the samples which had Fe_2O_3 precipitates were analysed by TEM using a JEM 200 CX transmission electron microscope.

The room-temperature EPR spectra of the samples were recorded by using a Varian E-112 EPR spectrometer operating at X-band frequencies ($\nu = 9.45$ GHz) having a 100 kHz first modulation and a phase-sensitive detection to obtain a field-derivative signal. DPPH was used as an internal standard ($g = 2.0036$).

The Mössbauer spectra were obtained on a conventional time-mode spectrometer (Wissel 1000 model) with constant acceleration drive and a triangular reference signal. A 10 mCi ^{57}Co in Rh matrix was used as radiation source. The data were collected in 256 channels and velocity calibration was performed with a natural iron foil of 25 μm thickness supplied by Amersham International plc. The absorber consisted of the finely ground samples spread out over the support in a uniform thickness of approximately 5 mg cm^{-2}. Spectra were run until an off-resonance count of nearly 5×10^6 was reached. The spectra were analysed by least-squares fittings [14] of Lorentzian lines to the data.

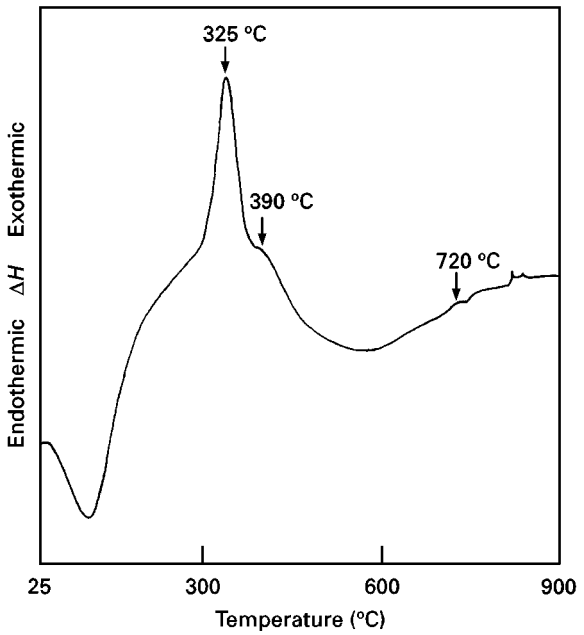

Figure 1 DTA curve for the oven-dried TiO_2–Fe_2O_3 specimen.

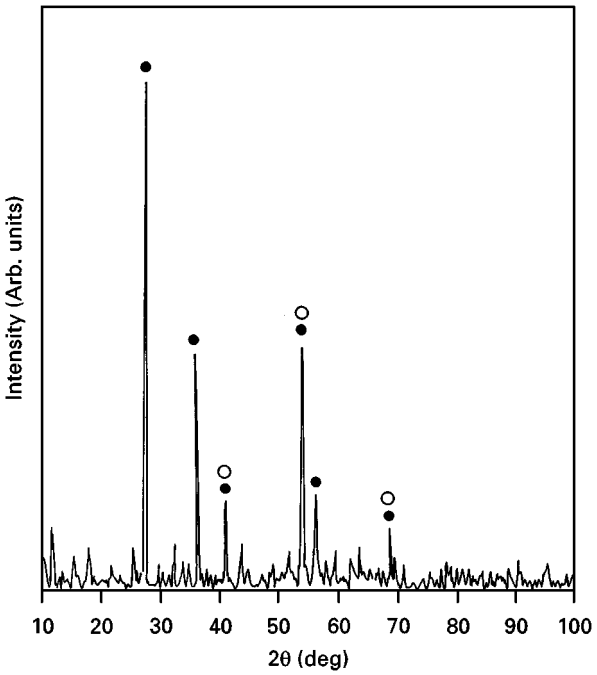

Figure 2 X-ray diffraction pattern of TiO_2–Fe_2O_3 specimen heated at 1000 °C for 2 h. (○) α-Fe_2O_3, (●) TiO_2.

3. Results and discussion

3.1. DTA analysis

Fig. 1 shows the DTA curve of the oven-dried sample. The curve showed two exothermic peaks at the temperatures 325 and 390 °C and one valley around 730 °C. The first peak was attributed to oxidation of the alkyl groups present in the gel because of an incomplete polycondensation reaction. The second one was due to the crystallization of anatase phase of TiO_2. This was evident from X-ray data and TEM analysis. The peak around 730 °C was believed to be due to the growth of α-Fe_2O_3 and TiO_2 rutile phases, respectively. This was also evident from the study of transmission electron micrographs.

3.2. X-ray diffractometry

The X-ray diffraction of the samples heated up to 600 °C showed the presence of anatase phase of TiO_2 whereas the rutile phase of TiO_2 and α-Fe_2O_3 appeared in the samples heated to higher temperatures, as summarized in Table I. The X-ray diffractrogram of sample F is shown in Fig. 2.

3.3. TEM analysis

Fig. 3 shows a transmission electron micrograph of the TiO_2–Fe_2O_3 sample heat treated at 1000 °C/2 h. Fig. 4 is the electron diffraction pattern of Fig. 3. The

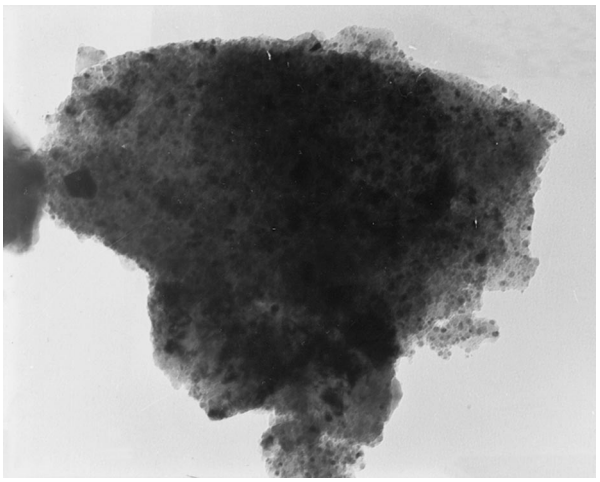

Figure 3 Transmission electron micrograph of sample TiO_2–Fe_2O_3 heat treated at 1000 °C for 2 h (× 100 000).

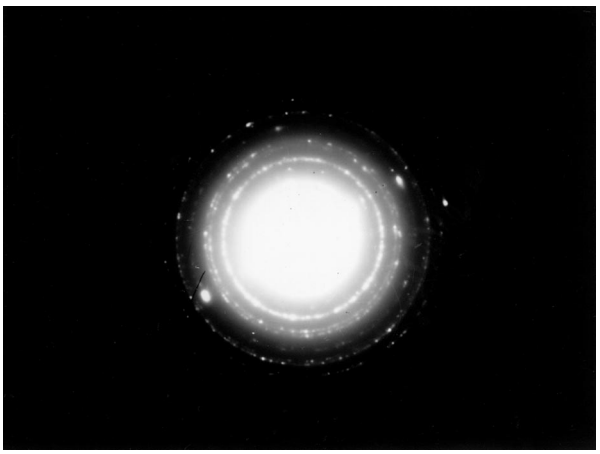

Figure 4 Electron diffraction pattern of Fig. 3.

TABLE II Comparison of interplanar spacings, d_{hkl}, for a specimen TiO_2–Fe_2O_3 heat treated at 1000 °C/2 h with standard ASTM data

d_{hkl} (nm) Observed	ASTM standard α-Fe_2O_3	ASTM standard TiO_2 (rutile)
0.1697	0.1690	0.1687
0.1477	0.1452	0.1480
0.1375	–	0.1360
0.1190	–	0.120
0.1060	0.1055	–
0.0941	0.0931	–

observed interplanar spacings, d_{hkl}, and standard data are compared in Table II. This confirms the presence of α-Fe_2O_3 and TiO_2 (rutile) phases, respectively. TEM of the samples heat treated at lower temperatures (< 800 °C) do not show the presence of any crystalline phase of iron, only confirms the presence of TiO_2 anatase phase which is evident from the diffraction ring analysis. In the sample heat treated above 800 °C, anatase TiO_2 phase is transformed to rutile TiO_2 phase. This is predicted from the corresponding diffraction ring analysis. These particles of TiO_2 are also of nanometre dimensions and are embedded in a glassy matrix. The results are summarized in Table I. Therefore, the samples heat treated above 800 °C are true nanocomposites containing both TiO_2 and α-Fe_2O_3 of nanometre dimensions. Fig. 5 is a typical histogram showing the particle-size distribution. The particle sizes analysed by the log normal distribution function [15] for different specimens, are given in Table III.

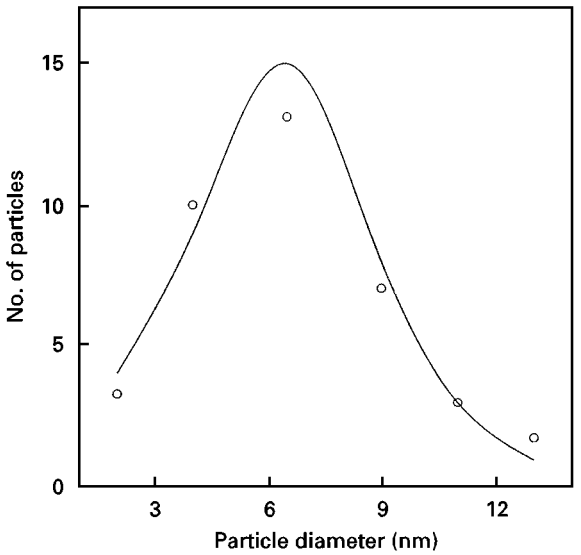

Figure 5 Histogram of nano-α-Fe_2O_3 grown in a titania matrix at 1000 °C for 2 h.

TABLE III Average particle size for different samples in the TiO_2–Fe_2O_3 system

Sample	Median particle diameter (nm)	Geometric standard deviation (nm)
E	4.0	1.5
F	6.2	1.6
G	10.0	1.2

3.4. EPR study

EPR spectra showed the presence of paramagnetic phase in all the samples. This was also evident from the Mössbauer study. EPR spectrum of sample F is given in Fig. 6. The peak having $g = 3.3922$ is typical of Fe^{3+} in a high-spin state.

3.5. Mössbauer analysis

Fig. 7 gives the Mössbauer spectrum for a sample subjected to a heat treatment at 600 °C for 2 h and Fig. 8 shows that for a sample heat treated at 1000 °C for 2 h. The continuous lines in these figures represent the computer-fitted results, whereas the dots represent the experimental data. The spectrum of sample D (Fig. 7) exhibits a symmetric quadrupole doublet showing the paramagnetic phase of the sample. The spectrum is fitted with one doublet resulting in the values of isomer shift and quadrupole splittings as 0.28 and 0.81 mm s^{-1}, respectively. This indicates that

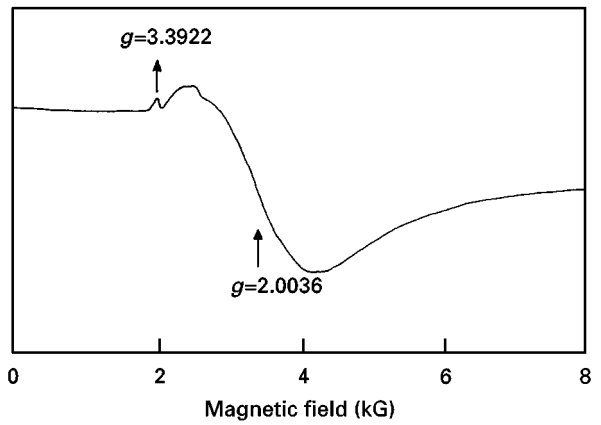

Figure 6 EPR spectrum of Fe_2O_3–TiO_2 nanocomposite heated at 1000 °C for 2 h.

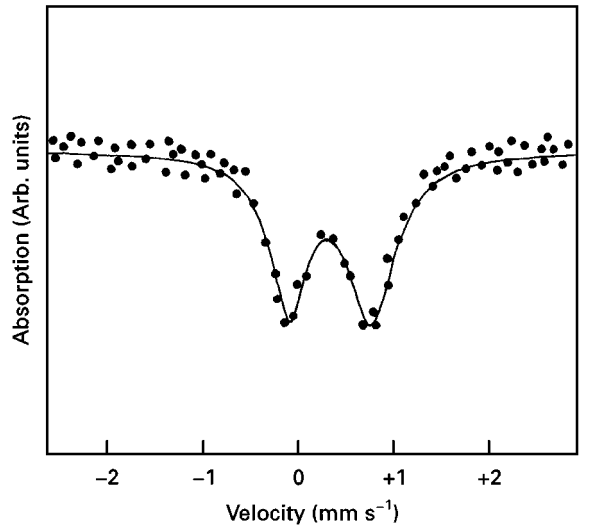

Figure 7 Room-temperature Mössbauer spectrum of sample TiO_2–Fe_2O_3 heat treated at 600 °C for 2 h.

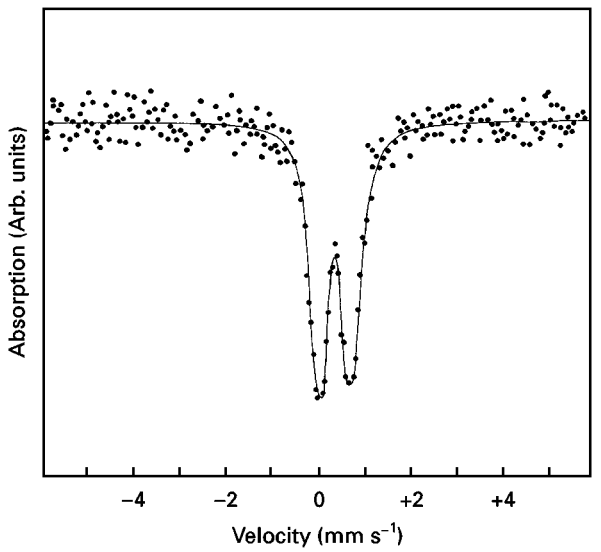

Figure 8 Room-temperature Mössbauer spectrum of sample TiO_2–Fe_2O_3 heat treated at 1000 °C for 2 h.

ferric ions prefer tetrahedral co-ordination in the amorphous iron titanate with high-spin configuration. We also took Mössbauer spectra of the samples A, B and C, but the data obtained did not show any significant difference with respect to that of sample D reported in Fig. 7. The spectrum of sample F (Fig. 8) shows an asymmetric doublet indicating the paramagnetic and superparamagnetic phase of nano-α-Fe_2O_3 in the sample, respectively. The spectrum is fitted with two doublets. It is to be noted that the Mössbauer spectrum of a magnetic nanocrystal is usually a superposition of a sextet corresponding to ferromagnetic particles with a superparamagnetic doublet corresponding to particles of smaller size. The particle size of the samples E, F and G increases with increasing heat-treatment temperature (Table III). The six magnetic lines of haematite are not present in the Mössbauer spectra of these samples. The value of isomer shift for the superparamagnetic doublet in the Mössbauer spectrum of the sample F (Fig. 8) is 0.34 mm s^{-1}, which is larger than those of the amorphous samples (A–D). These findings indicate the segregation of iron ions or finely divided superparamagnetic Fe_2O_3 particles as seen in the results from TEM.

4. Conclusions

Gel to glass transition was studied in the system TiO_2–Fe_2O_3 by thermal analysis. With increasing heat-treatment temperatures, larger particles of crystalline phases rutile and α-Fe_2O_3, respectively, precipitated within the glass medium. The particle diameter increased from 4 nm to 10 nm as the temperature was raised from 800 °C to 1150 °C. The nanocomposites exhibited superparamagnetic behaviour. The Mössbauer spectra of the samples consisted of paramagnetic and superparamagnetic doublets. We can conclude that there exists a critical size less than 10 nm in the case of α-Fe_2O_3, at which it becomes superparamagnetic in nature. Because of the large number of nucleation sites at the TiO_2/glass interface, the α-Fe_2O_3 particles grow to small sizes, i.e. diameters less than 10 nm. These α-Fe_2O_3 particles thus exhibit a superparamagnetic behaviour. But in the SiO_2–Fe_2O_3 system [13], the size of the α-Fe_2O_3 particles becomes larger with the same schedule of heat treatment and behave like a normal ferromagnetic species.

Acknowledgements

T.K. Kundu thanks CSIR, New Delhi, for the award of Senior Research Fellowship. The work was supported by a foreign research Grant no. N 00014-93-1-0040 by the office of Naval Research, Washington, USA.

References

1. D. CHAKRAVORTY and A. K. GIRI, in "Chemistry of Advanced Materials", edited by C. N. R. Rao (Blackwell Scientific, Oxford, 1992) p. 217.
2. A. CHATTERJEE and D. CHAKRAVORTY, *Appl. Phys. Lett.* **60** (1992) 138.
3. S. ROY, D. DAS, D. CHAKRAVORTY and D. C. AGRAWAL, *J. Appl. Phys.* **74** (1993) 4746.
4. T. K. KUNDU and D. CHAKRAVORTY, *J. Mater. Res.* **9** (1994) 2480.

5. J. P. WANG, D. H. HAN, H. L. LUO, N. F. GAO and Y. Y. LIU, *J. Magn. Magn. Mater.* **135** (1994) L251.
6. T. K. KUNDU and D. CHAKRAVORTY, *Appl. Phys. Lett.* **66** (1995) 3576.
7. C. G. GRANQVIST and O. HUNDERI, *Phys. Rev. B* **16** (1977) 3513.
8. B. ABELES, P. SHENG, M. D. COUTTS and Y. ARIE, *Adv. Phys.* **24** (1975) 407.
9. M. GUGLIELMI and G. PRINCIPI, *J. Non-Cryst. Solids* **48** (1982) 161.
10. Y. SHANG and G. V. WEERT, *Hydrometallurgy* **33** (1993) 273.
11. R. A. ROY and R. ROY, *Mater. Res. Bull.* **19** (1984) 169.
12. J. P. WANG and H. L. LUO, *J. Magn. Magn. Mater.* **131** (1994) 54.
13. T. P. SINHA, M. MUKHERJEE, D. CHAKRAVORTY and M. BHATTACHARYA, *Ind. J. Phys.* **70A** (1996) 741.
14. E. VON MEERWAL, *Computer Phys. Commun.* **9** (1975) 117.
15. B. ROY and D. CHAKRAVORTY, *J. Phys. Condens. Matter.* **2** (1990) 9323.

Received 29 April
and accepted 27 November 1997